NMR study of partial charge transfer in N-methylphenazinium-tetracyanoquinodimethane (NMP-TCNQ)

M. A. Butler and F. Wudl
Bell Laboratories, Murray Hill, New Jersey 07974

Z. G. Soos
Department of Chemistry, Princeton University, Princeton, New Jersey 08540
(Received 7 July 1975; revised manuscript received 25 August 1975)

The field dependence of the proton NMR second moment $M_2(H,T)$ of powder N-methylphenazinium-tetracyanoquinodimethane (NMP-TCNQ) and (DMP-TCNQ), the analogous material with a deuterated methyl, shows that at 4.2°K there are unpaired electrons localized on $\sim 6\%$ of the NMP sites. This strongly suggests partial ($\gamma = 0.94$) charge transfer in $NMP^{+\gamma}$-$TCNQ^{-\gamma}$, a room-temperature organic conductor previously thought to be fully ionic ($\gamma = 1$). The localized NMP moments are shown to be weakly coupled with a Weiss constant $\Theta \sim 0.6$°K, consistent with static susceptibility data. This local-moment picture is also consistent with the spin dynamics as indicated by low-temperature EPR measurements and the value of $M_2(0,4.2)$. At higher temperature $M_2(0,T)$ indicates a slowing down of spin fluctuations as T^{-1}, characteristic of one-dimensional systems. These results show cw NMR measurements with selective deuteration provide a useful method for determining the spatial distribution of spin susceptibility and thus the degree of ionicity γ. This is because *static* rather than dynamic magnetic properties are measured and as these interactions are well known, the interpretation of the data is simplified.

I. INTRODUCTION

Numerous physical techniques have recently been applied to quasi-one-dimensional organic "metals" in an effort to elucidate the physics of these conductors. Several recent reviews[1–5] summarize magnetic, electric, and optical studies in terms of theoretical models that are sometimes complementary, and sometimes incompatible. A major difficulty has been to obtain transport and dynamic properties for lower-dimensional models, a clear prerequisite for unambiguously analyzing various experimental results. Nuclear magnetic resonance (NMR) has been relatively infrequently applied to organic conductors, in spite of its demonstrated power for probing three-dimensional metals,[6,7] paramagnetic inorganic insulators,[8,9] and even paramagnetic organic semiconductors.[10–12] NMR studies[13,14] on organic conductors have typically focused on the nuclear spin-lattice relaxation time. Such dynamic properties inevitably require both a specific assumed model for the conductor and a fairly detailed knowledge of its solutions.

In this paper, we examine the role of continuous-wave (cw) NMR studies and present results for the one-dimensional organic conductor NMP-TCNQ,[15] whose constituent molecules are shown in Fig. 1. A major advantage of cw measurements is that *static* properties are probed. Since the elementary interactions between static magnetic moments are well known,[16,17] it is inherently simpler to compare theory and experiment. As shown below, our cw NMR data strongly suggest that NMP-TCNQ is not fully ionic, but has localized unpaired electrons associated with about 6% of the NMP sites. Such incomplete charge transfer has been previously suggested[3,18] for NMP-TCNQ and has generally been assumed[1,5] for the organic conductors related to TTF-TCNQ.[19] Nevertheless, it has been

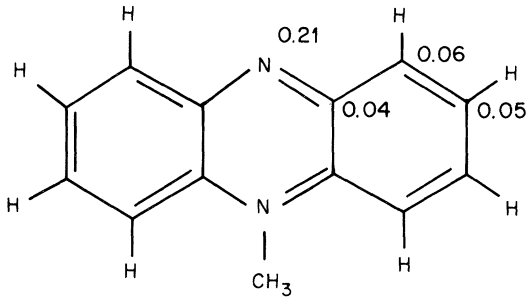

NMP

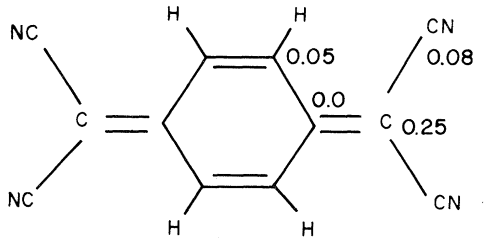

$TCNQ^-$

FIG. 1. Structure and π-electron spin densities for the neutral NMP radical and the $TCNQ^-$ anion radical. Magnitude of the spin densities is discussed in the text.

difficult to establish[20,21] the degree of ionicity in TTF-TCNQ and our results for partial charge transfer in NMP-TCNQ provide the first accurate determination of this important quantity. It is evident, for example, that previous theoretical models[22,23] in which all the paramagnetism was associated with a fully ionic $TCNQ^-$ stack in NMP-TCNQ must be reexamined.

It is instructive to examine the general advantages and limitations of cw NMR measurements on organic conductors by comparison with results for three-dimensional metals,[6,7] paramagnetic insulators,[8,9] and semiconductors.[10–12] In these systems information can be obtained from either the position of the resonance or from its shape. Paramagnetic shifts ΔH result from the polarization of the unpaired electron in a static magnetic field H and are given by

$$\Delta H/H = (A/g\mu_B)\chi , \tag{1}$$

where A is the hyperfine coupling constant, g is the g factor, μ_B is the Bohr magneton, and χ is the local static spin susceptibility. Such shifts occur in paramagnetic insulators[8,9,16,17] or semiconductors[10] in which the unpaired electrons are localized. Paramagnetic shifts also arise from conduction electrons in metals, Knight shifts, and have been studied[24] in the one-dimensional inorganic conductor, $K_2Pt(CN)_4Br_{0.3}3H_2O$.

Organic ion-radical solids contain unpaired electrons delocalized in π-molecular orbitals,[3] with reduced spin densities and small hyperfine coupling constants.[25] Paramagnetic shifts are consequently small. In addition, their measurement is further complicated by anisotropic, mainly dipolar, electron-nuclear interactions which are comparable in magnitude. The obvious advantages of using single crystals, as exploited in inorganic insulators,[8,9] is often difficult to achieve for organic conductors, owing to limitations of crystal size. Thus in powdered organic samples the NMR line is broadened by an amount comparable to the shift and accurate shift measurements become impractical.

Therefore we are led to consider the *shape* of the NMR absorption. Resonance line shapes are generally difficult to calculate even in ideal cases, especially in view of special effects[26] associated with lower dimensionality. A more useful, but also more limited, quantity that can be both measured and calculated with reasonable accuracy is the second moment,

$$M_2 = \int_{-\infty}^{\infty} (H - H_0)^2 f(H - H_0)\, dH , \tag{2}$$

where $f(H - H_0)$ is the observed absorption centered at H_0 and H is the applied field. The temperature and field dependence of the second moment for powder samples of NMP-TCNQ are presented in Sec. II, and the analysis of M_2 will provide evidence both for partial transfer in NMP-TCNQ and for the distribution of the unpaired electrons. Considerable information can be obtained from second-moment analyses as shown by their exploitation in early works.[16,27,28]

The occurrence of small paramagnetic shifts and the frequent necessity of using powder samples are major inconveniences for cw studies on organic conductors. Only ^1H can readily be used among the nuclei commonly found in organic systems (i.e., H, C, N, O). The other nuclei either have a very small natural abundance of isotopes with spin or have sizable quadrupolar interactions, which would broaden the resonance in a powder sample. ^1H has $I = \frac{1}{2}$ and thus no quadrupole moment. These limitations can be overcome by isotope enrichment (e.g., ^{13}C) and/or by sizable ($\gtrsim 10^{21}$ spin) single crystals. However, such procedures are difficult. Selective deuteration offers a more fruitful course of action. For example, the CH_3 group of NMP in Fig. 1 can readily be replaced[14] by a CD_3 group to yield N-deuteromethylphenazinium (DMP). Deuteration enables one to identify the origins of the remaining ^1H absorption and, as shown below, the DMP-TCNQ results are important in determining the distribution of unpaired electrons in NMP-TCNQ.

Our choice of NMP-TCNQ as a representative organic conductor for exploring cw NMR methods was based on several considerations. First, NMP-TCNQ was an early[29] example of a highly conducting organic solid. Its structure is relatively simple,[30] although recent developments[31,32] point to the existence of multiple phases, a common feature of stacked organic solids.[3] Second, NMP-TCNQ has been extensively studied[1–5,22] and has provided detailed applications for contrasting theoretical models. Third, NMP-TCNQ is, at low temperature, a paramagnetic semiconductor whose properties are expected to be more easily interpreted. Finally, our interest[3,33] in partial charge transfer is especially straightforward to test in NMP-TCNQ. Complete transfer corresponds to diamagnetic NMP^+ ions and paramagnetic $TCNQ^{-1}$ ion radicals, while less than complete transfer necessarily implies some paramagnetism on the NMP sites also.

We present in Sec. II second-moment NMR results for powdered NMP-TCNQ and DMP-TCNQ, the analog with a deuterated methyl group in Fig. 1, and identify the internuclear contribution. The field dependence of the second moment is combined with static susceptibility data in Sec. III to show a 6% concentration of localized magnetic moments on NMP and DMP. Several independent determinations of the degree of charge transfer are

presented. The zero-field electronic contributions to the second moment are related to spin fluctuations in Sec. IV. The resulting zeroth-order model for NMP-TCNQ is briefly discussed in Sec. V.

II. NMR RESULTS

NMP-TCNQ samples were prepared by the procedure discussed in Refs. 29 and 22. No extensive procedures were attempted to "purify" the material, as such methods affect primarily the conductivity.[34] Small single crystals recrystallized from spectrograde CH_3CN showed a narrow (ΔH ~0.15 G) EPR line at X-band at 300 °K. DMP-TCNQ was prepared by reacting phenazine with hexadeutero-dimethyl sulfate (99+% deuterated), followed by exchange of the methosulfate anion for the TCNQ anion under standard[29] conditions. No loss of deuterium was observed from the methyl group when DMP-TCNQ was treated with CF_3CO_2H, filtered, and the resultant DMP^+ solution's NMR was recorded.

The cw NMR experiments were performed using a standard bridge spectrometer and signal averaging techniques. The temperature was determined by cryogenic liquids or a nitrogen gas flow system. Powder samples of about 0.2–0.3 g were convenient. Figure 2 shows a typical spectrum for DMP-TCNQ at 77.3 °K.

The occurrence of structure in Fig. 2 is evident and the line is accurately represented as a pair of Gaussians split by ~3 G. This type of spectrum is expected[27,28] for protons occurring in pairs, since dipolar interactions for protons 2.4 Å apart produce a 3-G splitting. As shown in Fig. 1, the TCNQ protons occur in pairs at a separation of 2.24 Å,

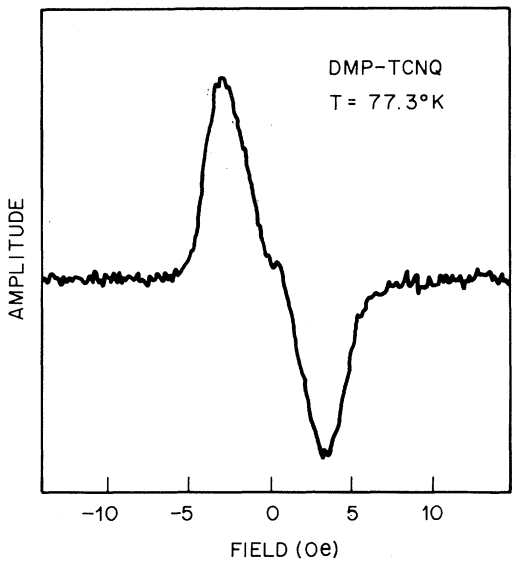

FIG. 2. cw NMR derivative spectrum for DMP-TCNQ powder at 77.3 °K.

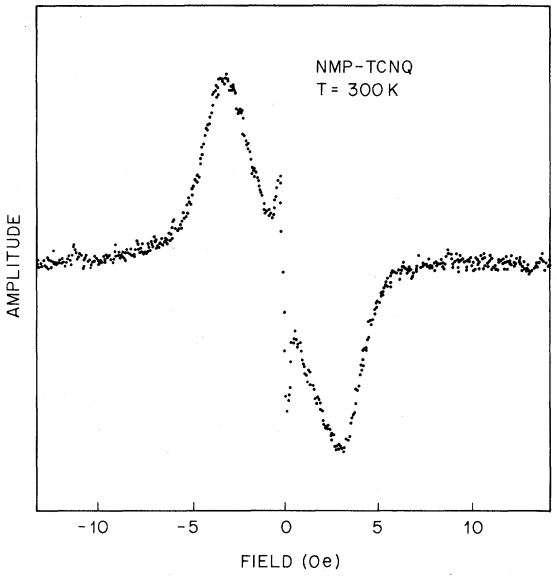

FIG. 3. cw NMR derivative spectrum for NMP-TCNQ powder at 300 °K. Note the sharp central component to the resonance.

while the DMP protons occur in groups of four at a separation of 2.45 Å. Consideration of the linear four-spin problem indicates that these protons also produce a spectrum dominated by a doublet, with a splitting representative of the proton-proton separation. The NMP-TCNQ spectrum is also best represented as a pair of Gaussians split by ~3 G, but the obvious structure seen in the DMP-TCNQ in Fig. 2 is obscured, presumably by the CH_3 contribution to the proton resonance. The observed spectra are therefore consistent with the known nuclear dipolar fields in the solid.

The room-temperature resonance shown in Fig. 3 for NMP-TCNQ has an additional sharp [full width half-maximum (FWHM) < 0.5 G] line superimposed at the center. This resonance was observed in all our samples of NMP-TCNQ (which came from several different batches prepared by different people over a period of several years) and DMP-TCNQ. Its integrated intensity is ~0.5% at 300 °K. Upon cooling the resonance broadens and disappears at ~230 °K. The narrow line indicates rapid proton motion. To remove the possibility of absorbed solvent (CH_3CN), a deuterated CD_3CN solvent was used, but the resonance remained. Such sharp resonances have been observed[35] previously in organic solids and were attributed to premelting phenomena or incipient sample decomposition. We have not assigned these sharp high-temperature resonances. Their contribution to the second moment is entirely negligible in any case.

The formal expression (2) for the second moment M_2 is in terms of the absorption function $f(H)$ rather than in terms of the derivative $f'(H)$

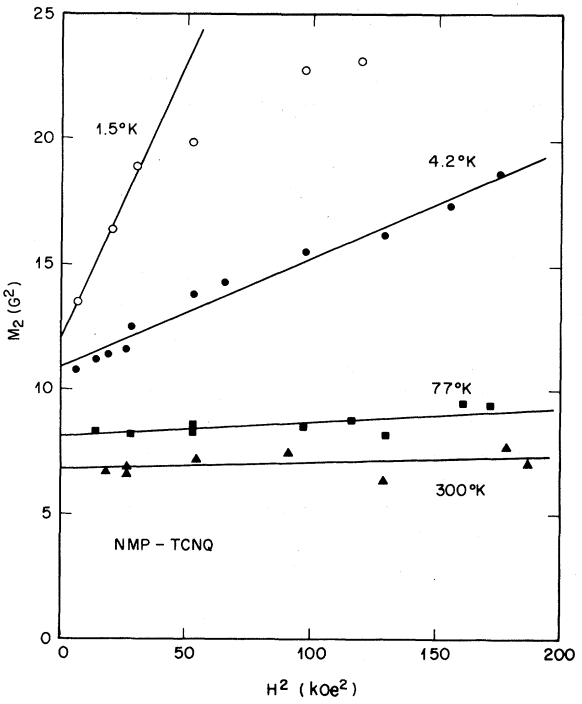

FIG. 4. Field dependence of the measured second moment $M_2(H, T)$ in NMP-TCNQ powder at various temperatures. Straight line is a least-squares fit to Eq. (5); 1.5 °K data are discussed in the text.

shown in Figs. 2 and 3. An integration by parts yields

$$M_2 = \tfrac{1}{3}(H - H_0)^3 f(H)\Big|_{-\infty}^{\infty} - \frac{1}{3}\int_{-\infty}^{\infty} (H - H_0)^3 f'(H - H_0)\, dH \,. \tag{3}$$

The first term vanishes, while practical considerations limit the integration in the second term to some cutoff α. The experimentally determined second moment is therefore

$$M_2(H, T) = -\frac{1}{3}\int_{H_0-\alpha}^{H_0+\alpha} (H' - H_0)^3 f'(H' - H_0)\, dH' \,, \tag{4}$$

and is a function of both the applied field and temperature.

There exists an optimum value for the cutoff α. Large α includes more of the complete second moment but also worsens noise fluctuations, which are amplified by the $(H - H_0)^3$ factor. The appropriate value of α was found by generating an artificial spectrum, based on a known (Gaussian) line shape, with a Gaussian noise spectrum yielding a signal-to-noise ratio (S/N) of 100. This is a typical S/N value in our experiments and involves a varying amount of signal averaging depending on the temperature. It was found that numerical integration of the data with $\alpha = 16$ G provided the best compromise with noise problems and yet gave M_2 values good to ~5%.

The field dependence of $M_2(H, T)$ for NMP-TCNQ is shown in Fig. 4. The solid lines are least-squares fits to

$$M_2(H, T) = M_2(0, T) + B(T)H^2 \,, \tag{5}$$

where $B(T)$ will be related to the local static susceptibility and $M_2(0, T)$ contains various dipolar contributions. The least-squares fits to the points in Fig. 4 indicate a weak field dependence even at 77 and 300 °K. These may result from instrumental effects, as the magnet inhomogeneities are greater at high fields. The 4.2 °K data clearly illustrate an H^2 dependence. Deviations from linearity at 1.5 °K probably reflect cutoff errors, as a larger cutoff $\alpha = 20$ G gives a larger M_2 and a more linear behavior in H^2. The strong temperature dependence of the paramagnetic susceptibility at low temperature, both in our and in other[22,36-38] NMP-TCNQ samples, will be related to the temperature dependence of $B(T)$.

The temperature dependences of $M_2(0, T)$ for both NMP-TCNQ and DMP-TCNQ are shown in Fig. 5 and illustrate the effects of partial deuteration.[14] The different values of $B(T)$ for NMP-TCNQ and DMP-TCNQ at 4.2 °K are shown in Fig. 6. Such a difference in the field dependence of $M_2(H, T)$ is a direct clue for the occurrence of unpaired spins, and thus of a local electronic susceptibility on the NMP part of the lattice.

The NMP-TCNQ crystal structure[30] is based

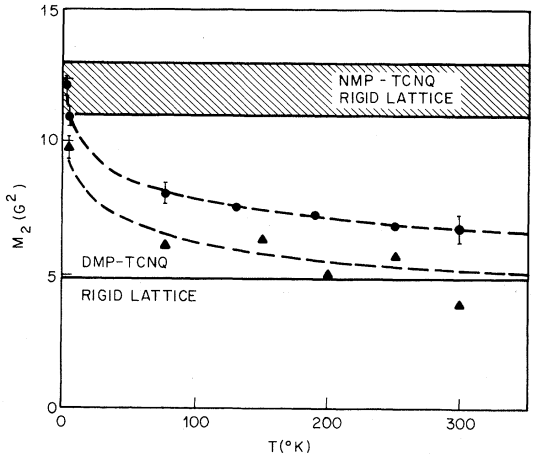

FIG. 5. Measured and calculated zero-field second moments $M_2(0, T)$ for DMP-TCNQ and NMP-TCNQ. Circles are NMP-TCNQ and the triangles DMP-TCNQ. Rigid lattice for NMP-TCNQ is based on several hypothetical orientations for a nonrotating methyl group. Points with error bars are an average of several runs. Those without have an error of ~10%. Dashed lines are smoothed curves through corresponding sets of data points separated by 1.5 G^2 to show the corresponding increases in DMP-TCNQ and NMP-TCNQ.

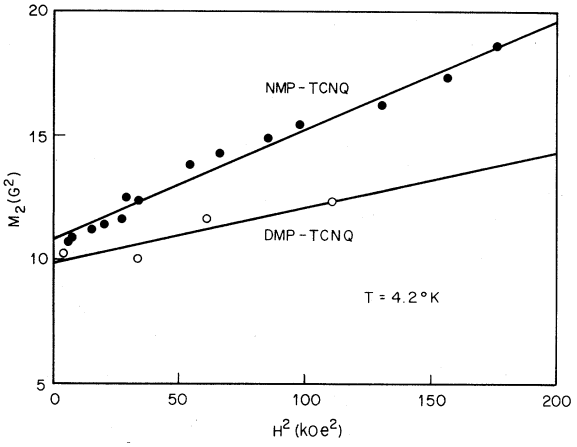

FIG. 6. Field dependence of the measured second moment $M_2(H, T)$ for NMP-TCNQ and DMP-TCNQ at 4.2 °K. Lines are least-squares fits to Eq. (5).

on parallel segregated stacks of planar NMP^+ and $TCNQ^-$ molecules along the a axis, as shown in Fig. 7. The disorder of the CH_3 group of NMP, which could be attached to either N, is in question now that an ordered phase has been observed.[31] Other features of the structures were identical. Small crystals from our samples did not show methyl ordering[32] and were consistent with the previous disordered structure. While the crystal structure is important for interpreting the second-moment data, the exact position of the methyl group is not. It clearly plays no role at all in DMP-TCNQ. All dipolar sums in Eqs. (6) and (7) are based on atomic coordinates from Fritchie's structure.[30]

The dipolar interactions between protons provide a well-known[16,17] contribution to $M_2(0, T)$. The nuclear dipolar contribution to the jth proton in the unit cell is, for a powder sample, in units of G^2,

$$M_2^j = \tfrac{3}{5}\gamma_n^2\hbar^2 I(I+1)\sum_k{}' r_{jk}^{-6}, \qquad (6)$$

where γ_n is the gyromagnetic ratio, $I=\frac{1}{2}$, and the truncated dipolar interaction is summed over all other protons at r_{jk}. For N_p protons in the unit cell, the nuclear dipolar broadening is

$$M_2^{n-n} = \frac{1}{N_p}\sum_{j=1}^{N_p} M_2^j \qquad (7)$$

and, as shown in Fig. 5, correctly accounts for the DMP-TCNQ data. The NMP-TCNQ data in Fig. 5 are evidence[14] for rapid methyl rotation about the C–N axis at all temperatures, since the observed $M_2(0, T)$ are substantially below the rigid-lattice value. Reduction of the methyl contribution is well known[27,28,35] and leads to reasonable agreement with $M_2(0, T)$ at high temperature.[14] While the nuclear-nuclear contribution to the second moment provides no information about the electronic states, the agreement between theory and experiment at high temperature does provide a check on the moment measuring procedure, since no adjustable parameters are used.

Since slowing down of the methyl rotation would affect the behavior of $M_2(0, T)$ only in NMP-TCNQ, the observed temperature dependence of $M_2(0, T)$ for both NMP-TCNQ and DMP-TCNQ must reflect electron-nuclear interactions in these paramagnetic solids. The nearly parallel behavior in Fig. 5 points to a common electronic origin. Electron-nuclear interactions would in fact dominate $M_2(0, T)$, were it not for rapid spin fluctuations[16] that reduce this contribution. A discussion of spin fluctuations requires some model for spin dynamics and is consequently postponed until a zeroth-order picture of NMP-TCNQ has been formulated purely on the basis of static properties.

III. LOCALIZED NMP MOMENTS

We turn next to the field dependence of $M_2(H, T)$ shown in Figs. 4 and 6. The application of a uniform magnetic field H to a paramagnetic system polarizes the electronic moments. The average polarization $\langle S_i\rangle$ for the ith spin produces a local field h_i which in turn can broaden or shift the resonances of nearby nuclei.

We therefore seek to compute the local electronic fields produced at the nuclear site j. There are two contributions. Isotropic hyperfine interac-

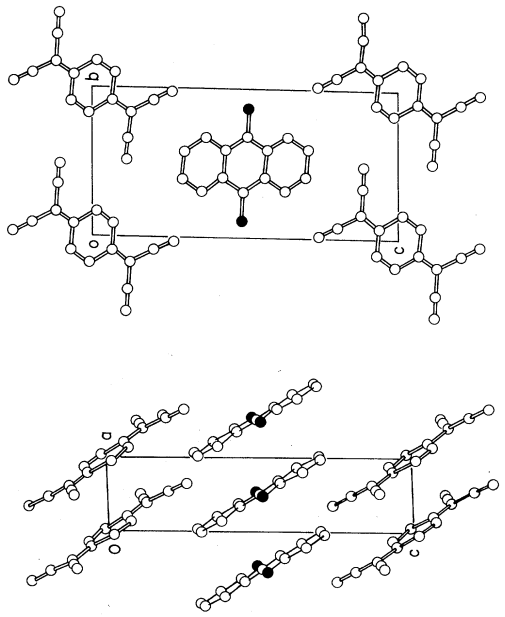

FIG. 7. NMP-TCNQ crystal structure from Ref. 30. The disordered methyl group (●) can be attached to either nitrogen.

tions yield

$$h_j^h = a_j \chi_j H , \tag{8}$$

where a_j is the coupling constant and χ_j is the local electronic susceptibility on the molecule to which the jth proton belongs. Compilations[25,39,40] of hyperfine coupling constants are available from solution EPR data on π-electron ion radicals. The second electronic contribution to the local field at the jth proton is the truncated dipolar interaction

$$h_j^d = \sum_i (3\cos^2\theta_{ij} - 1) r_{ij}^{-3} \rho_i \chi_i H , \tag{9}$$

where the sum is over electronic moments at r_{ij}, θ_{ij} is the angle between $\vec{r}_{ij}$ and $\vec{H}$, and ρ_i is the spin density on the ith atom. The spin densities at the various atoms are indicated in Fig. 1 for $TCNQ^-$ and involve both solution EPR and approximate theoretical results.[39] NMP^+ is diamagnetic, with $\chi_i = 0$. However, NMP is paramagnetic, with 15 π electrons, and its spin densities indicated in Fig. 1 are based on the related 15-π-electron systems, nine methyl anthracene negative ion[41] and dihydrophenazine positive ion.[42] The powder average of Eq. (9) vanishes, while the hyperfine contribution [Eq. (8)] can shift the resonance even in a powder.

Since the electronic and nuclear spins are uncorrelated at the temperature of interest here, their contributions to the proton second moment are additive. The field-dependent electronic contribution is just the mean-square deviation of the local fields,

$$B(T)H^2 = \frac{1}{N_p} \sum_j^{N_p} [(h_j^d)^2 + (h_j^h)^2] - \left(\frac{1}{N_p} \sum_j^{N_p} h_j^h \right)^2 , \tag{10}$$

where N_p is the number of protons in the unit cell and we have used the fact that the powder average of h_j^d vanishes. The proportionality of both h_j^d and h_j^h to the applied field H immediately accounts for the H^2 dependence of $M_2(H, T)$ seen in Figs. 4 and 6. The temperature dependence of χ_i leads to a temperature dependence of $B(T)$.

Although the general features of the field dependence of $M_2(H, T)$ are easily understood qualitatively, a detailed model for the distribution of the electronic moments must be assumed for a quantitative treatment. As all parameters are known except the distribution of the spin susceptibility, we can test various assumed distributions by computing $B(T)$ in Eq. (10). The key factor is the different $B(4.2)$ for NMP-TCNQ and DMP-TCNQ shown in Fig. 6. This provides a stringent test of any model without having to rely on absolute agreement between calculated and measured values.

There are many simple TCNQ salts with diamagnetic counterions[3] and they are semiconductors. Although NMP-TCNQ is a conductor, the obvious starting point is again to assume complete charge transfer, with diamagnetic NMP^+ sites and a half-filled $TCNQ^-$ stack. The spin susceptibility is uniformly distributed in the proposed[22] Hubbard model. The $TCNQ^-$ coupling constant is[39] $a_j = 1.58$ G and the spin susceptibility in our sample was found to be $(7.66 \pm 0.48) \times 10^{-27}$ emu/molecule at 4.2 °K by using the Schumacher-Slichter[43] method of Ref. 22. The calculated value of $B(4.2)$ from Eq. (10) is about twice as large as measured for NMP-TCNQ and is even further from the DMP-TCNQ value. More important, a uniform spin susceptibility on $TCNQ^-$ does not give the different slopes for NMP-TCNQ and DMP-TCNQ in Fig. 6, and is consequently decisively ruled out. The reason is that the $TCNQ^-$ protons dominate $M_2(H, T)$ and the protons on diamagnetic NMP^+ sites are relatively unimportant. Localization of the unpaired electrons on one, or a few, $TCNQ^-$ sites, which is characteristic of the disorder model,[5,23] is also ruled out by the different $B(4.2)$ values for NMP-TCNQ and DMP-TCNQ. Without any adjustable parameters, cw NMR data thus indicate that all the pramagnetism at 4.2 °K cannot be associated with the TCNQ stack. This assumption was the starting point for previous models[22,23] of NMP-TCNQ, which consequently require reexamination.

Since methyl coupling constants are generally larger[10,25] than those of ring protons in π molecular systems, assigning the observed susceptibility to a uniform distribution on the NMP stack (i.e., postulating a neutral NMP-TCNQ lattice and diamagnetic TCNQ sites) leads to even poorer numerical agreement with $B(4.2)$. Such a model, nevertheless, provides a strong dependence on CH_3 deuteration. Since we do not expect a neutral NMP-TCNQ lattice on chemical grounds, we are led to postulate a limited number of local moments on an NMP stack and to consider a model in which these local moments dominate the spin susceptibility at 4.2 °K.

In particular, we introduce a parameter γ to describe the degree of ionicity[3] for $NMP^{+\gamma}$-$TCNQ^{-\gamma}$. Clearly $\gamma < 1$ corresponds to less than complete transfer of charge. The resulting concentration $(1 - \gamma)$ of unpaired electrons on the NMP stack is treated as localized $S = \frac{1}{2}$ moments that are at most weakly interacting with each other and with the $TCNQ^{-\gamma}$ spins. The local susceptibility is then

$$\chi_{loc} = g^2 \mu_B^2 / 4k(T + \Theta) , \tag{11}$$

where g is very close to the free-electron g value of 2.0023 in these π-electron radicals and the Weiss constant Θ describes small interactions with the

local moments. The spin susceptibility associated with a concentration of $1-\gamma$ NMP sites is just $(1-\gamma)\chi_{1oc}$. It is emphasized that the form (11) for χ_{1oc} was chosen for its simplicity. Lower-temperature χ data has been interpreted[2] by a different power law. In either case the local moments are weakly interacting.

To describe the NMR results, we assume a spatial distribution for the local moments on the NMP stack. Complete localization on a single site is not consistent with χ data and the analysis will be carried out for delocalization on two adjacent NMPs. A similar treatment can be used for any degree of delocalization. Although both a uniform paramagnetism and complete localization can be ruled out, the exact degree of delocalization to a few sites must remain somewhat flexible on the basis of the present results.

We then consider protons on two adjacent NMP sites containing an unpaired electron obeying a Curie-Weiss susceptibility, with small Θ in Eq. (11). In a 10-kG field, the 4.2 °K hyperfine shifts [Eq. (8)] are ~45 and 125 G for ring and methyl protons, respectively. These protons are well outside the cutoff α for the M_2 integration (4). In addition, they are likely[16,44] to be rapidly relaxed and broadened by the electronic moment. In short, we would not expect to observe the protons on localized paramagnetic sites, whether $TCNQ^-$ or NMP, both because they are greatly shifted and greatly broadened.

Protons not on the NMP site are shifted by the electron dipolar field, which decreases as r^{-3} and is within the cutoff limits even for adjacent sites. Since there are no hyperfine shifts for protons not on the NMP sites, the contribution of the localized NMP moments to $B(T)$ in Eq. (10) are given entirely by the powder average of the dipolar fields h_i^d in Eq. (9). For $1-\gamma$ small we compute the contributions from a single NMP spin to be

$$B_{\mathrm{NMP}}(T)H^2 = \frac{1}{NN_p}\sum_j (h_j^d)^2 = \frac{\chi_{1oc}^2}{NN_p}\ \frac{2}{5}\sum_{jik} r_{jk}^{-3} r_{ji}^{-3}\rho_i\rho_k(3\cos^2\theta_{ik}-1)H^2 . \tag{12}$$

Here N is the number of unit cells in the solid, j sums over all protons in the solid except those on the paramagnetic NMP site,

$$\cos\theta_{ik} = (\vec{r}_{ij}\cdot\vec{r}_{kj})/|\vec{r}_{ij}|\cdot|\vec{r}_{kj}| ,$$

and the i and k sums are over the NMP atoms with spin densities indicated in Fig. 1. The total contribution to $B(T)$ from the $(1-\gamma)N$ localized NMP moments is, for $1-\gamma \ll 1$, just

$$B_{1oc}(T) = (1-\gamma)\chi_{1oc}^2\ \frac{1}{N_p} \times \frac{2}{5}\sum_{ijk}\rho_i\rho_k r_{ij}^{-3} r_{ik}^{-3}(3\cos^2\theta_{ik}-1) . \tag{13}$$

The sum in Eq. (13) has been evaluated numerically for the NMP-TCNQ lattice[30] and the NMP spin densities in Fig. 1. The result is $1.91\times10^{45}\ \mathrm{cm}^{-6}$ for NMP-TCNQ and $1.17\times10^{45}\ \mathrm{cm}^{-6}$ for DMP-TCNQ. As shown below, the NMP susceptibility of $(1-\gamma)\chi_{1oc}$ corresponds to essentially all the observed χ at 4.2 °K. Thus we neglect $TCNQ^{-\gamma}$ contributions to $\chi(4.2)$.

The assignment of the observed $B(4.2)$ in Fig. 6 as due to B_{1oc} in Eq. (13) now allows several comparisons for testing the model of localized NMP sites. The ratio of the NMP-TCNQ and DMP-TCNQ slopes in Fig. 6 allows a *no parameter* test. The theoretical ratio (for the same value of $1-\gamma$) is

$$\frac{1.91/15}{1.17/12} = 1.31$$

since $N_p = 15$ for NMP-TCNQ and 12 for DMP-TCNQ. The experimental slopes are $(4.3\pm0.3)\times10^{-8}$ for NMP-TCNQ and $(2.2\pm0.7)\times10^{-8}$ for DMP-TCNQ. Their ratio is 1.9 ± 0.5.

In order to minimize the possible sample dependence[38] of χ, we used the Schumacher-Slichter[22] method to determine χ in the same samples for which $M_2(H, T)$ data were available. The 4.2 °K results were $(7.66\pm0.48)\times10^{-27}$ emu/molecule for NMP-TCNQ and $(7.01\pm0.23)\times10^{-27}$ emu/molecule for DMP-TCNQ. These results are consistent with the same value of $1-\gamma$ in both samples. However, if we use $\chi_{\mathrm{meas}} = (1-\gamma)\chi_{1oc}$ in Eq. (13) and thus allow slightly different γ values, the calculated ratio of slopes in 1.6 ± 0.3, with the errors associated with the susceptibility measurement, in satisfactory agreement with the experimental ratio of 1.9 ± 0.5.

This agreement encourages us to examine further the model of moments localized to adjacent NMP sites. The measured values of $B(4.2)$ and of $\chi_{\mathrm{meas}} = (1-\gamma)\chi_{1oc}$ provide, through a rearrangement of Eq. (13), an expression for the concentration, $1-\gamma$, of NMP sites

$$1-\gamma = \frac{2}{5}\ \frac{\chi_{\mathrm{meas}}^2}{B(4.2)}\ \frac{1}{N_p}\sum_{ijk}\rho_i\rho_k r_{ij}^{-3} r_{kj}^{-3}(3\cos^2\theta_{ik}-1) . \tag{14}$$

The results are $(6.9\pm1.4)\%$ for NMP-TCNQ and $(8.2\pm3.3)\%$ for DMP-TCNQ. Thus we have some 6% of localized NMP sites in either case. There are again no adjustable parameters.

Such a low concentration of local moments and small χ contributions from the $TCNQ^{-\gamma}$ stack require a small Weiss constant Θ in Eq. (11). A small Θ will also be indicated by EPR results. Again neglecting the $TCNQ^{-\gamma}$ contribution to the slope $B(T)$ at 4.2 or 1.5 °K, we have

$$\frac{B(1.5)}{B(4.2)} = \frac{\chi_{1oc}^2(1.5)}{\chi_{1oc}^2(4.2)} = \left(\frac{4.2+\Theta}{1.5+\Theta}\right)^2 . \quad (15)$$

The measured slopes of $(4.3 \pm 0.3) \times 10^{-8}$ and $(22.4 \pm 2.0) \times 10^{-8}$ at 4.2 and 1.5 °K, respectively, for NMP-TCNQ yield $\Theta \sim 0.6$ °K. The localized moments are almost, but not quite, decoupled from each other and from magnetic moments on the $TCNQ^{-\gamma}$ chain. As shown below such weak interactions are sufficient to exchange narrow any hyperfine or dipolar splittings of the localized sites.

A further check on the value of $1-\gamma$ is possible by using $\chi_{meas} = (1-\gamma)\chi_{1oc}$ and $\Theta = 0.6$ °K in Eq. (11). In effect, the static susceptibility must correspond to *at least* the Curie-Weiss contribution of the local moments. Assuming no contribution from $TCNQ^{-\gamma}$, we find $1-\gamma = (5.9 \pm 0.4)\%$ for NMP-TCNQ and $(5.4 \pm 0.2)\%$ for DMP-TCNQ. This justifies our previous neglect of the $TCNQ^{-\gamma}$ contribution at $T = 4.2$ or 1.5 °K and provides another determination of $1-\gamma$.

One could of course attempt[36] to partition χ_{meas} into various contributions such as local moments and $TCNQ^{-\gamma}$ contributions. This is a difficult procedure on account of the scatter in the χ data shown in Fig. 8 for our and others NMP-TCNQ samples. Indeed, χ data has generally not been useful in organic ion radicals for establishing the correct zeroth-order model,[3] but rather has served as a check. The log-log plot in Fig. 8 leads to a slope of -1 for a Curie law, or for a Curie-Weiss law when $T \gg \Theta$, as shown by the solid line for 6% local moments and $\Theta = 0$. The dashed line in Fig. 8 results for adding a temperature-independent contribution determined from the 300 °K value. It is evident that the "other" contributions are very sensitive to the exact value of $1-\gamma$ and that identifying their contribution by subtraction would be questionable even if there were no scatter in the χ data. The static susceptibility of NMP-TCNQ may in fact be sample dependent.[38] It is worth noting the reasonable agreement between our Schumacher-Slichter and more conventional χ results at 4.2 °K. This indicates that essentially all the protons are observed in the NMR experiment as required for $1-\gamma \ll 1$.

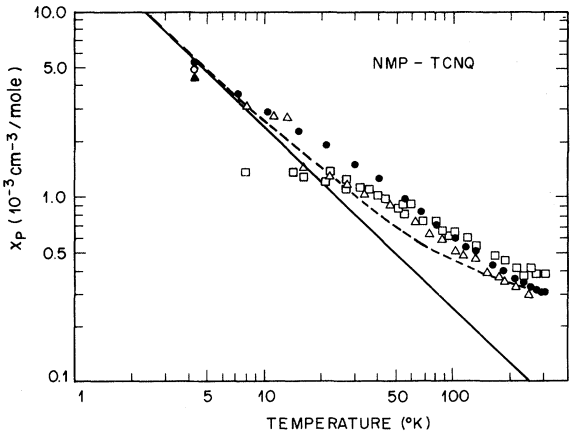

FIG. 8. Log-log plot of static susceptibility at NMP-TCNQ corrected for diamagnetic contributions. ● are Di Salvo's results for our samples; △ are from Ref. 36; □ are Schumacher-Slichter data from Ref. 22; ○ and ▲ are 4.2 °K Schumacher-Slichter results for our NMP-TCNQ and DMP-TCNQ, respectively.

The consistency of results with the static susceptibility data points to the model of some 6% localized electrons on the NMP stack at 4.2 °K in our NMP-TCNQ and DMP-TCNQ samples. In addition, both the slopes of $M_2(H, T)$ vs H^2 and χ data provide several independent determinations of $1-\gamma = (6 \pm 2)\%$. Our NMR data are thus consistent with about 94% charge transfer in NMP-TCNQ.

IV. SPIN FLUCTUATIONS

Until now we have focused entirely on *static* magnetic properties, and especially on the field dependence of $M_2(H, T)$, to establish the existence of localized NMP moments in our samples of NMP-TCNQ and DMP-TCNQ. The only model assumption introduced was to localize some moments. We now examine some of the implications of this model for the dynamics of the spin system. In particular, we consider the temperature dependence of $M_2(0, T)$ shown in Fig. 5 and relate it to a common electronic origin in both NMP-TCNQ and DMP-TCNQ.

Since the $TCNQ^{-\gamma}$ spins are sufficiently strongly interacting to make a negligible contribution to χ at 4.2 °K, we consider the measured second moment at this temperature, where our model should be applicable. The principal *dynamic* electron-nuclear interaction at 4.2 °K is the dipolar interaction with the randomly distributed localized NMP spins. They correspond to a magnetically dilute[45] system. Indeed the observed χ in various organic ion-radical crystals without random moments can be used to define a uniform magnetic dilution[3,46] which accounts phenomenologically for the temperature, pressure, and even angular dependence of exchange-narrowed EPR lines. Magnetic dilution leads to a scaling of second moments. The powder average for time-dependent dipolar interactions between unlike spins[16,17] is thus scaled by the concentration, $1-\gamma$, of NMP spins to yield

$$M_2^{n-e} = (1-\gamma)\tfrac{1}{3} g^2 \mu_B^2 S(S+1) \times \frac{2}{5} \frac{1}{N_p} \sum_{ijk} \rho_i \rho_k r_{ij}^{-3} r_{kj}^{-3} (3\cos^2\theta_{ik} - 1) . \quad (16)$$

The sum has already been discussed and evaluated in connection with Eq. (13). For $1-\gamma \sim 6\%$, M_2^{n-e}

is more than 100 G^2, far larger than the observed M_2. Rapid spin fluctuations can, of course, reduce the electronic contribution to yield an exchange or motionally narrowed[16,46] Lorentzian line of width

$$\Gamma = M_2^{n-e}\tau_c , \tag{17}$$

where τ_c is a typical electronic fluctuation time. As has been emphasized,[26] care must be taken with the simple formula (17) in one-dimensional systems, where it may be considerably in error. There is no *a priori* reason for invoking the high-temperature limit, for which the spin dynamics are partly known,[26] in quasi-one-dimensional organic ion-radical solids[3]; also, the coupling of the local moments may be three dimensional in nature. Thus, we use the crude approximation (17) as a preliminary estimate for the spin correlation time τ_c.

The cutoff α introduced in the second-moment analysis limits the contribution from the wings of the Lorentzian. Consideration of the convolution of Gaussian and Lorentizan lines, for a Gaussian linewidth small compared to the cutoff α, gives the following expression for the experimental NMR second moment:

$$M_2(0, T) = M_2^{n-n} + (2\alpha/\pi) M_2^{n-e}\tau_c . \tag{18}$$

Here M_2^{n-n} is the Gaussian interproton contribution given in Eq. (7) and $(2\alpha/\pi) M_2^{n-e}\tau_c$ is the truncated Lorentzian. Since M_2^{n-n} is independent of temperature, the increased value of $M_2(0, 4.2)$ shown in Fig. 5 provides an estimate for τ_c. For M_2^{n-e} ~ 245 G^2 and $\alpha = 16$ G, we have $\tau_c \sim 10^{-10}$ sec for both NMP-TCNQ and DMP-TCNQ. The corresponding rate, $\omega_c = \tau_c^{-1} = 10^{10}$ sec^{-1} is of the order of the Weiss constant $\Theta = 0.6$ °K found from the temperature dependence of $B(T)$.

Thus the dynamical properties of the localized spins in our model are also consistent. These local moments can also be observed by EPR and $\tau_c \sim 10^{-10}$ sec enters in the EPR linewidth of ~ 0.3–0.5 G at 4.2 °K. The local moment contribution to M_2^{e-e} is reduced[45] by $1-\gamma$ from the hypothetical fully paramagnetic value of roughly 4×10^4 G^2 (for dipolar fields of $\sim 2\times10^2$ G in stacked π-molecular solids).[47] Thus we expect the 4.2 °K value of M_2^{e-e} to be about 10^3 G^2 for some 6% localized NMP spins. A correlation time of $\tau_c = 10^{-10}$ sec then gives a narrowed EPR line of less than 1 G from Eq. (17). The precise distribution of spins is important in estimating M_2^{e-e} and we must consider the order-of-magnitude agreement satisfactory.

At higher temperatures the $TCNQ^{-\gamma}$ spins make a major contribution to χ and provide[46] and additional temperature-dependent electron-nuclear contribution to M_2^{n-e}. The temperature dependence of $M_2(0, T) - M_2^{n-n}$ in Fig. 9 shows that the electronic contribution to M_2 for both NMP-TCNQ and DMP-TCNQ decreases as T^{-1}. Thus the spin correlation time τ_c is decreasing as T^{-1}. While many systems exhibit such a temperature dependence, it is worth noting that one-dimensional systems quite generally exhibit slow decay of correlations[48] and, in particular, the linear Heisenberg chain[49] decays as T^{-1}.

Single-crystal EPR studies[50,51] on NMP-TCNQ will undoubtedly permit a far more detailed analysis of the spin dynamics. Our purpose here was to show show that the spin dynamics, as exemplified by the value of $M_2(0, 4.2)$ and the qualitative features of the EPR spectrum, are consistent with the zeroth-order model of a few percent of localized NMP spins that are weakly coupled to each other and/or to the $TCNQ^{-\gamma}$ spins.

V. DISCUSSION

In view of the small hyperfine shifts in organic molecules and the frequent limitations to powder samples, we have focused on the second moment (2) of the NMR line rather than on paramagnetic shifts. It is evident that the NMP-TCNQ results were made possible by the relatively large low-temperature electronic susceptibility. This susceptibility was associated with a 6% concentration of localized NMP moments.

NMP-TCNQ does not, apparently, undergo a

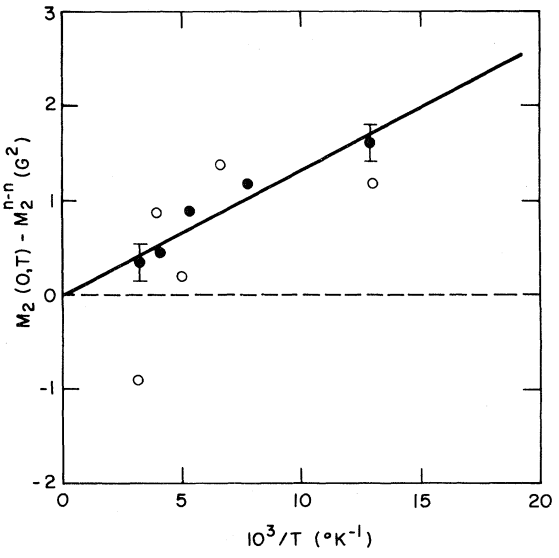

FIG. 9. Temperature dependence of the electronic contribution to the second moment, $M_2(0, T) - M_2^{n-n}$ in Eq. (18), for NMP-TCNQ (●) and DMP-TCNQ (○). Straight line is a least-squares fit of the NMP-TCNQ data to T^{-1}.

structural change between its low-temperature region of paramagnetic insulator and its high-temperature region of high conductivity. Thus the results of partial transfer at 4.2 °K could hold at higher temperature. Nevertheless, the NMR analysis does not provide direct evidence for or against partial transfer above 77 °K. By 77 °K, as shown in Fig. 4, the field dependence of $M_2(H, T)$ is quite small. The susceptibility is greatly reduced and is no longer dominated by the localized moments. Thus a highly accurate measurement of the slope of $M_2(H, T)$ obtained by going to higher fields, while maintaining good homogeneity, would be more difficult to interpret. Both NMP and $TCNQ^{-\gamma}$ spins now contribute to χ and care must be exercised in determining which protons contribute to the resonance. However, further selective deuteration (i.e., complete deuteration of NMP or of TCNQ) would enable a separation of the various contributions. In addition, the advantage afforded by selective deuteration can be used to delineate the susceptibility distribution in TTF-TCNQ and any other complex system.

We have used spin distributions for $TCNQ^-$ based on solution data and have approximated the NMP spin distribution in Fig. 1 by those of related ions. There is considerable EPR evidence[3] from semiconducting π-molecular crystals that such solution spin densities are not appreciably changed in the solid state. We have also used NMP spin distributions obtained from Huckel calculations.[52] Only small changes were found, since the greatest spin densities remain on the N atoms. While N-ethylphenazine is a stable neutral free-radical solid,[53] the neutral NMP radical has yet to be prepared, and experimentally determined spin densities are not available. Such data would not alter the conclusion of $6 \pm 2\%$ localized NMP moments in NMP-TCNQ.

In view of the possible controversy about sample purity[1,34] and multiple phases[31,32] in NMP-TCNQ, the present NMR data may not describe all samples. However, there is little doubt that the paramagnetism is indeed associated with localized NMP moments in our samples at 4.2 °K. Since our conclusions are based on low-temperature data, we cannot rule out additional possibilities. First, a temperature-dependent degree of charge transfer can, of course, be made to fit the χ data in Fig. 8. All that is needed is to have a slowly increasing concentration of local moments. Second, the remote possibility that some of the NMP was inadvertently protonated, to form N-methylhydrophenazinium cation radicals in the solid, cannot be ruled out by NMR alone and such a small (1 H for 6% of the NMPs) excess would be difficult to detect by chemical analysis. It is well worth emphasizing that the failure of several solid-state models for NMP-TCNQ lies precisely in not allowing for the novel possibility of partial charge transfer. Thus NMR data at 4.2 °K indicate some 6% of localized spin on NMP and strong interactions in the $TCNQ^{-\gamma}$ stack, but do not otherwise restrict the zeroth-order model. The interpretation[54] of other data on NMP-TCNQ will provide a more complete picture.

There is direct structural evidence[32] that our NMP samples contain disordered methyl groups, as originally proposed.[30] A very attractive combination of these results is to associate localized NMP moments with "misfit" NMP molecules whose methyl group, and dipole moment, is incorrectly oriented relative to its neighbors. Such a model would provide the two equivalent sites over which to localize the electrons. The large dipole-dipole repulsion energy would be reduced.[55] Such a polarization contribution must, in fact, be invoked to rationalize the existence of NMP-TCNQ, since the direct electrostatic contributions to the Madelung energy turn out to be very small.[56] "Misfit" molecules would naturally be sensitive to the crystallization condition. The χ data in Fig. 8 show a substantial, but variable increase at low temperature, which is consistent with localized NMP sites. These changes, of the order of several percent NMP, are an order of magnitude larger than errors in chemical purity.

The most important consequence of less than complete charge transfer in NMP-TCNQ is to point to the requirement of complex TCNQ systems in achieving high conductivity. This was suggested in early conductivity work[57] and recently on the basis of optical data.[18] A compilation[3] of stacked π-molecular ion-radical systems also supports the importance of complex (or either more or less than one conduction electron per site) stacks for high conductivity. NMP-TCNQ, TTF-TCNQ, and its relatives were the only 1:1, or apparently simple conductors. Partial transfer leads to complex systems of the type $NMP^{+\gamma}$-$TCNQ^{-\gamma}$, or $TTF^{+\gamma}$-$TCNQ^{-\gamma}$, with $\gamma \neq 1$. The occurrence of high conduction in uniform complex system is then consistent with experiment and can readily be understood even for strong correlations.[3] When there are fewer conduction electrons than sites, conduction can occur without double occupancy and thus at low energy. There is no gap for the special case of the less than half-filled Hubbard model.[58] Similarly, more than one electron per site again allows for low-energy conduction, since there is no need to change the number of doubly occupied sites.

In summary, the low-temperature NMR data for NMP-TCNQ indicate some $1 - \gamma \sim 6\%$ of localized NMP sites and consequently a less than half-filled $TCNQ^{-\gamma}$ stack. The field dependence of the

NMR second moment for NMP-TCNQ and DMP-TCNQ rules out a uniform low-temperature paramagnetism and permits a direct evaluation of the degree of ionicity γ from purely static considerations. The charge and spin dynamics of NMP-TCNQ will require additional analysis of the zeroth-order model of incomplete charge transfer indicated by NMR.

ACKNOWLEDGMENTS

We thank F. J. DiSalvo and W. M. Walsh for access to unpublished work, and A. J. Silverstein, D. L. Blockus, and M. Kaplan for valuable technical assistance. One of us (Z. G. S.) gratefully acknowledges support from the National Science Foundation, Grant No. GP-4302.

[1]H. J. Keller, *Low-Dimensional Cooperative Phenomena* (Plenum, New York, 1975). The contributed papers provide a good general introduction to various types of one-dimensional systems.

[2]I. F. Shchegolev, Phys. Status Solidi A 12, 4 (1972).

[3]Z. G. Soos, Ann. Rev. Phys. Chem. 25, 121 (1974); Z. G. Soos and D. J. Klein, in *Molecular Associations*, edited by R. Foster (Academic, New York, 1975). A general development and compilation of charge-transfer systems is given, including the more numerous semiconducting and insulating TCNQ salts.

[4]A. F. Garito and A. J. Heeger, Acc. Chem. Res. 7, 232 (1974). See also A. J. Heeger and A. F. Garito in Ref. 1.

[5]A. N. Bloch, in *Charge and Energy Transfer in Organic Semiconductors*, edited by K. Masuda and M. Silver (Plenum, New York, 1974), p. 159.

[6]J. Winter, *Magnetic Resonance in Metals* (Clarendon, Oxford, 1971).

[7]A. Narath, in *Hyperfine Interactions*, edited by A. J. Freeman and R. B. Frenkel (Academic, New York, 1967), p. 287.

[8]D. Hone, C. Scherer, and F. Borsa, Phys. Rev. B 9, 965 (1974); J. P. Boucher, F. Ferrieu, and M. Nechtschein, *ibid.* 9, 3871 (1974).

[9]T. O. Klaassen, S. Wittekoek, J. J. Van der Klink, and N. J. Poulis, Physica (Utr.) 41, 523 (1969); S. Wittekoek, Ph.D. thesis (Leiden, 1967) (unpublished); A. Kawamori and G. Soda, Mol. Phys. 29, 1085 (1975).

[10]A. Kawamori and T. Suzuki, Mol. Phys. 8, 95 (1964).

[11]G. Nyberg, D. B. Chesnut, and B. Crist, J. Chem. Phys. 50, 341 (1969); G. M. Semeniuk and D. B. Chesnut, Chem. Phys. Lett. 25, 251 (1974).

[12]F. Devreux and M. Nechtschein, Solid State Commun. 16, 275 (1975).

[13]E. Ehrenfreund, E. F. Rybaczewski, A. F. Garito, and A. J. Heeger, Phys. Rev. Lett. 28, 873 (1972); E. F. Rybaczewski, A. F. Garito, A. J. Heeger, and E. Ehrenfreund *ibid.* 34, 524 (1975).

[14]M. A. Butler, F. Wudl, and Z. G. Soos (unpublished).

[15]NMP-TCNQ is N-methylphenazinium-tetracyanoquinodimethane.

[16]A. Abragam, *The Principles of Nuclear Magnetism* (Clarendon, Oxford, 1961), Chaps. IV, VI, and X.

[17]C. P. Slichter, *Principles of Magnetic Resonance* (Harper and Row, New York, 1963), Chaps. 3 and 4.

[18]J. B. Torrance, B. A. Scott, and F. B. Kaufman, Solid State Commun. (to be published).

[19]TTF is tetrathiafulvalene.

[20]W. D. Grobman, R. A. Pollak, D. E. Eastman, E. T. Mass, Jr., and B. A. Scott, Phys. Rev. Lett. 32, 534 (1974). This technique has been questioned by A. J. Epstein, N. O. Lipari, P. Nielsen, and D. J. Sandman, Phys. Rev. Lett. 34, 914 (1975).

[21]M. A. Butler, J. P. Ferraris, A. N. Bloch, and D. O. Cowan, Chem. Phys. Lett. 24, 600 (1974).

[22]A. J. Epstein, S. Etemad, A. F. Garito, and A. J. Heeger, Phys. Rev. B 5, 952 (1972). See Ref. 1 for the failure of a half-filled Hubbard model description of the $TCNQ^-$ chain to give the observed magnetic susceptibility of NMP-TCNQ.

[23]A. N. Bloch, R. B. Weisman, and C. M. Varma, Phys. Rev. Lett. 28, 753 (1972). See also Ref. 5. The most detailed application of the disorder model to NMP-TCNQ is given by V. Walatka, Jr., Ph.D. thesis (Johns Hopkins University, 1973) (unpublished).

[24]H. J. Keller and H. H. Rupp, Z. Naturforsch. A 26, 785 (1971); See also H. Launois and H. Diedoba in Ref. 1.

[25]A. Carrington, Q. Rev. Chem. Soc. 17, 67 (1963).

[26]D. W. Hone and P. M. Richards, Ann. Rev. Mater. Sci. 4, 337 (1974). Special line-shape effects are emphasized by P. M. Richards in Ref. 1.

[27]H. S. Gutowsky and G. E. Pake, J. Chem. Phys. 18, 162 (1950).

[28]E. R. Andrew, J. Chem. Phys. 18, 607 (1950); E. R. Andrew and R. Bersohn, *ibid.* 18, 159 (1950).

[29]L. R. Melby, Can. J. Chem. 43, 1448 (1965).

[30]C. J. Fritchie, Jr., Acta Crystallogr. 20, 892 (1965).

[31]H. Kobayashi, Bull. Chem. Soc. Jpn. 48, 1373 (1975).

[32]B. Morosin, Phys. Lett. A 53, 455 (1975). A second nonmagnetic phase of NMP-TCNQ has been reported by L. B. Coleman, S. K. Khanna, A. F. Garito, A. J. Heeger, and B. Morosin, Phys. Lett. A 42, 15 (1972).

[33]D. J. Klein, W. A. Seitz, M. A. Butler, and Z. G. Soos (unpublished).

[34]L. B. Coleman, A. J. Cohen, A. F. Garito, and A. J. Heeger, Phys. Rev. B 7, 2122 (1973).

[35]H. M. McIntyre and C. S. Johnson, Jr., J. Chem. Phys. 55, 345 (1971); J. G. Powles and H. S. Gutowsky, *ibid.* 21, 1695 (1953).

[36]I. F. Shchegolev, L. I. Buravov, A. V. Zvarykina, and R. B. Lynbovskii, Zh. Eksp. Teor. Fiz. 8, 353 (1968) [Sov. Phys.-JETP 28, 218 (1968)].

[37]K. Siratori and T. Kondow, J. Phys. Soc. Jpn. 27, 301 (1969).

[38]M. H. Cohen (private communication) has collected other unpublished recent susceptibility results on NMP-TCNQ; they all show a strong variable increase at low temperature.

[39]P. H. Rieger and G. K. Fraenkel, J. Chem. Phys. 37, 2795 (1962); H. T. Jonkman and J. Kommandeur, Chem. Phys. Lett. 15, 496 (1972). Spin densities for π-molecular ion radicals are also collected by R. M. Metzger, Ph.D. thesis (California Institute of Technology, 1969) (unpublished).

[40]A Carrington and J. Dos Santos-Veiga, Mol. Phys. 5, 615 (1962).

[41]J. R. Bolton, A. Carrington, and A. D. McLachlan,

Mol. Phys. 5, 31 (1962).
[42]K. H. Hausser, A. Habich, and V. Franzen, Z. Naturforsch. A 16, 836 (1961).
[43]R. T. Schumacher and C. P. Slichter, Phys. Rev. 101, 58 (1956).
[44]K. A. Hausser and D. Stehlik, Adv. Magn. Reson. 3, 79 (1968). In general, it is quite difficult to observe protons at paramagnetic sites.
[45]C. Kittel and E. Abrahams, Phys. Rev. 90, 238 (1953).
[46]Z. G. Soos, J. Chem. Phys. 46, 4284 (1967). See also Z. G. Soos in Ref. 1.
[47]T. Z. Huang, R. P. Taylor, and Z. G. Soos, Phys. Rev. Lett. 28, 1054 (1972).
[48]P. Pincus in Ref. 1.
[49]F. B. McLean and M. Blume, Phys. Rev. B 7, 1149 (1973).
[50]Y. Tomkiewicz (private communication).
[51]W. M. Walsh (private communication).
[52]R. M. Metzger (private communication). While it is necessary to delocalize the electrons in π-molecular systems, small variations in the spin or charge densities at the various atomic sites do not affect either the fine structure calculations (Ref. 3) or Madelung energy calculations; see R. M. Metzger, J. Chem. Phys. 57, 1876 (1972).
[53]H. McIlwain, J. Chem. Soc. 1704 (1937); K. Hausser and J. N. Murrell, J. Chem. Phys. 27, 500 (1957).
[54]Z. G. Soos, in *Highly Conducting Organic Materials*, edited by F. Wudl (Academic, New York, to be published).
[55]D. J. Klein (private communication).
[56]R. M. Metzger, J. Chem. Phys. 57, 2218 (1972).
[57]W. J. Siemons, P. E. Bierstedt, and R. G. Kepler, J. Chem. Phys. 39, 3523 (1963).
[58]A. A. Ovchinnikov, Zh. Eksp. Teor. Fiz. 57, 2137 (1969) [Sov. Phys.-JETP 30, 1160 (1970)].